

# Molecular modelling of interactions at the composite interfaces between electrolytically surface-treated carbon fibre and epoxy resin

Ian Hamerton,<sup>a</sup> John N. Hay,<sup>a</sup> Brendan J. Howlin,<sup>a</sup> John R. Jones,<sup>a</sup> Shui-Yu Lu,<sup>\*a</sup> Graham A. Webb<sup>a</sup> and Michael G. Bader<sup>b</sup>

<sup>a</sup>Department of Chemistry, University of Surrey, Guildford, UK GU2 5XH

<sup>b</sup>Department of Materials Science and Engineering, University of Surrey, Guildford, UK GU2 5XH

Two carbon fibre models, based on microscopic and XPS evidence of electrochemical surface treatment, have been proposed. A diagonal graphitic plane, comprising 52 six-membered rings (in a 4 × 13 configuration) and of 150 carbon atoms, was built as the principal, non-surface-treated carbon fibre model. Three layers of graphitic planes, each comprising 117 six-membered rings (in a 9 × 13 configuration) and of 300 carbon atoms, formed the multi-layer graphitic model. The nature and level of surface treatment was represented by the introduction of hydroxy (OH) and carboxy (COOH) groups: each time, a C—C bond was broken along the edge of the plane, and a pair of OH and COOH groups was added to the graphitic plane. Six pairs of OH and COOH were introduced gradually. The functional groups were distributed evenly along the edge of each graphitic plane. Their non-covalent bonding interaction with various amine-cured epoxy polymer models was simulated using the Cerius<sup>2</sup> BLENDS method.  $\Delta_{\text{mix}}G$  was used to indicate the interaction, and hence the interfacial adhesion. The results show a trend, in relation to the level of surface treatment, in agreement with experimental data of composite interlaminar shear strength (ILSS).

Epoxy resins are important engineering matrix materials for polymeric composites reinforced by carbon fibres, and the most common of these is the diglycidyl ether of bisphenol A (DGEBA). Reinforcement in such composites is only achieved by sufficient stress transfer between the fibres and the matrix; such stress transfers can be realised by mechanical interlocking, physical adhesion and chemical bonding.<sup>1</sup> Despite its importance, the nature of the interphase region in fibre-reinforced polymers remains largely unresolved. Wright<sup>2</sup> has prepared an extensive review of the literature data of the properties of the carbon fibre/epoxy resin interphase. He considered a variety of factors including carbon fibre surface treatment and its effect on fibre and composite properties, the use of different sizes and polymer coatings and their effect on composite properties, and theoretical approaches and experimental techniques for the study of the interphase region. The standard technology to improve stress transfer within composites consists of surface treatment of the fibres by various oxidation treatments. The improvement of the interlaminar shear strength (ILSS) of carbon fibre-reinforced polymer (CFRP) with a DGEBA matrix and surface-treated carbon fibres is evident in many research papers.<sup>3</sup> Wright remarked that all carbon fibre surface treatments appear to be oxidative in nature, possibly leading to increased fibre surface area, removal of a weak surface layer, and modification of the surface chemistry. All three phenomena serve to improve resin wetting and bonding, and of these the available evidence suggests that the change in surface area is not a significant parameter, although the polar surface Gibbs energy was found to increase on treatment. Surface analysis using X-ray photoelectron spectroscopy (XPS) showed that acidic surface groups, such as phenolic and carboxylic functional groups, were introduced as a result of the surface treatment.<sup>4</sup>

The use of molecular modelling is widespread in the pharmaceutical industry for drug design and has met with considerable success. Increasingly, there is a need to understand the properties and features of polymeric materials at the molecular level. Recent advances have enabled the method to predict the properties of structural, electromagnetic and optical materials.<sup>5–8</sup> However, few simulations have been carried out in the

area of composite interfacial properties: Attwood and Marshall<sup>9</sup> investigated theoretical differences in adsorption behaviour (*i.e.* adsorption energy,  $\Delta_{\text{ad}}H$ ) of the two major components [tetraglycidyl diaminodiphenylmethane, TGDDM, and bis(4-aminophenyl)sulfone, DDS] in an epoxy resin system. The carbon fibre surface model was constructed with reference to data provided by XPS. Trends obtained from the modelled data were corroborated by inverse gas chromatography (IGC) data. They recognised the model's limitation due to its inability to account accurately for the redistribution of charges during the minimisation process. Nevertheless the calculated adsorption energies of 35.4 kcal mol<sup>-1</sup> (1 cal = 4.184 J) for TGDDM and 23.6 kcal mol<sup>-1</sup> for DDS support an earlier hypothesis that TGDDM is attracted more strongly to the surface of HTA carbon fibres than DDS. Calderone *et al.*<sup>10</sup> undertook a series of theoretical calculations on model systems of well defined structure in order to determine the most favourable conformations of the polyethylene and polystyrene chains on a graphite-like surface and to rationalise the polymer/carbon interfacial interaction. The polyethylene/graphite and polystyrene/graphite interfaces were modelled by complexes formed by benzene with methane, ethane or propane or with ethylbenzene, respectively. They concluded that the *ab initio* calculation indicated that the alkane/benzene and ethylbenzene/benzene systems form van der Waals complexes, with large intermolecular separations leading to binding energies of the order of a few kcal mol<sup>-1</sup> per polymer repeat unit. The empirical molecular mechanics techniques lead in many instances to similar conformations and binding energies to those obtained with the *ab initio* method.

In the present work we are seeking to increase our understanding of the complex nature of the fibre-reinforced composite at its interfaces using molecular modelling. Two carbon fibre models, based on microscopic,<sup>11</sup> XPS<sup>4</sup> and quantitative surface functional group analytical evidence<sup>12</sup> of electrochemical surface treatment, were proposed, and their non-covalent bonding interactions with various amine-cured epoxy polymer models were investigated using the BLENDS method. The results were compared with the experimental data of composite interfacial strength, published by Marshall *et al.*<sup>13</sup> and Baillie and Bader.<sup>14</sup>

## Calculations

A Silicon Graphics Indy workstation (MIPS R4000) running the computer program Cerius<sup>2</sup> v1.6 (Molecular Simulations Inc.) was used to generate models of monomer, polymer and graphitic planes for models of the carbon fibre. In all the plates, atoms are represented by different colours, *e.g.* light grey for carbon, red for oxygen, green for nitrogen, yellow for sulfur and white for hydrogen. H atoms are not all shown in the plates in most cases. Some nitrogen atoms are highlighted as green balls.

### Molecular simulation method

The property prediction method, BLENDS, was used to investigate the interactions between two macromolecules. The module combines a modified Flory–Huggins model and molecular simulation techniques to calculate the compatibility of binary mixtures. The theoretical and computational considerations were developed by Blanco and co-workers.<sup>15</sup> These mixtures range from small molecules to large macromolecular systems, including polymer solutions, polymer blends and alloys. The information obtained includes phase diagrams (binodal and spinodal curves), thermodynamic mixing variables (enthalpy, entropy, change in Gibbs energy), the temperature-dependent interaction parameter,  $\chi(T)$ , binding energy component analysis, and the identification of favourable binding configurations between species, such as molecular pairs, molecules and surfaces, additives and bulk materials, and liquids and crystals.<sup>16</sup> The Dreiding 2.21 force field, as described elsewhere,<sup>17</sup> was used in this work. The charge calculation method, the charge equilibration ( $Q_{eq}$ ),<sup>18</sup> was used to assign, edit and calculate point charges.

In implementing the Flory–Huggins lattice model for polymers, BLENDS requires that the lattice sites be occupied by polymer segments. BLENDS is also an off-lattice calculation, meaning that molecules are not arranged on a regular lattice as in the original Flory–Huggins theory. In practice, each of the graphitic models and the polymer models occupies one lattice site. The degrees of polymerisation  $X_1$  and  $X_2$  were both set to 1, and the total molecular masses of the polymers were ignored.

BLENDS also provides options that place restrictions on both molecule alignment and atom contact during packing, and thus allows one to obtain more representative interaction energies of  $ij$  pairs,  $E_{ij}$  values. Graphitic structures in carbon fibres are highly oriented, therefore models are aligned along the principal axes. The allowed range of orientation was 10°. On the other hand, the epoxy polymer models have an isotropic (random) packing with no restrictions at all.

The interaction parameter,  $\chi(T)$ , is defined as:

$$\chi(T) = \frac{E_{\text{mix}}(T)}{RT} = \frac{(Z_{12}E_{12} + Z_{21}E_{21} - Z_{11}E_{11} - Z_{22}E_{22})}{2RT} \quad (1)$$

$E_{ij}$  is the interaction energy for a pair of molecules  $ij$ . BLENDS uses Monte Carlo atomistic simulations both to generate thousands of different molecular orientations and to calculate their pair-interaction energies. This method results in four Boltzmann-averaged  $E_{ij}$  values.  $Z_{ij}$ , the coordination number, is the number of molecules of type  $j$  that can be packed around a single molecule of type  $i$ . A single coordination number has a definite physical significance only when two components of the binary mixture have a similar volume or surface area.  $Z$  is calculated explicitly for each of the possible molecular pairs using a molecular simulation method called nearest-neighbours packing. This involves generating clusters in which nearest neighbours are packed around the central molecule until no more will fit. The van der Waals surfaces are used to represent the shape of the molecules. We matched the single-layer graphitic model (150 atoms) with polymer models comprising

10 repeat units (about 200 atoms). However, the polymer chain size was not changed in the multi-layered model calculation because of computing time restrictions.

BLENDS analysis options can be used both to calculate thermodynamic functions (entropy, enthalpy and Gibbs energy of mixing) for a binary system, and to create plots of these functions *vs.* composition at a specific temperature. The plots generated reflect the current choice of the interaction parameter model,  $\chi(T)$ , and the degree of polymerisation of the two components [see eqn. (2)].

$$\frac{\Delta_{\text{mix}}G}{RT} = \frac{\phi_1}{X_1} \ln \phi_1 + \frac{\phi_2}{X_2} \ln \phi_2 + \chi \phi_1 \phi_2 \quad (2)$$

where  $\Delta_{\text{mix}}G$  is the Gibbs energy of mixing,  $\phi$  is the volume fraction of each component, and  $X_1$  and  $X_2$  are the degrees of polymerisation (or chain length) of each component.

The plots of thermodynamic isotherms showed that  $\Delta_{\text{mix}}G$  is sensitive to changes in the volume fraction, but not to temperature in the range 300–400 K. Therefore the interaction between the carbon fibre model and the polymer is characterised by  $\Delta_{\text{mix}}G$ . This was calculated from  $\phi_1 = \phi_2 = 0.5$ , and at  $T = 300$  K as a typical example.

### Basic considerations on carbon fibre model construction

The production of PAN-based carbon fibres results from the carbonisation of the organic precursor, polyacrylonitrile (PAN), which is spun into fibre. The degree of graphitisation and microporosity, as indicated by their densities (1.7–1.9 g cm<sup>-3</sup> compared with 2.1 g cm<sup>-3</sup> for graphite), varies for different types of carbon fibres, *e.g.* high tensile, high strength and high modulus, depending on the carbonisation temperature. Elemental analysis (XPS) showed the presence of residual nitrogen in the carbon fibres, indicating that the carbonisation process was not always complete.<sup>4</sup> Johnson<sup>11</sup> suggested that there was no evidence of skin/core structure in high-modulus, high-strength, PAN-based carbon fibres, and that effects noted previously were caused by internal stress and etching effects, or by a varying radius of curvature of the crystal planes. He proposed a lamellar model with interlinked layer planes in all directions. Guigon and Oberlin<sup>19</sup> continued with the observation that curved crystal planes exhibit a skin effect for most high-modulus fibres, but stated that some high-modulus fibres have a skin/core structure. They proposed a microstructure model of a high tensile strength fibre which compares reasonably well with that of Johnson.<sup>11</sup> A mosaic pattern of graphite crystals 50–150 nm long but less than six atoms (2 nm) thick has also been observed.<sup>20</sup>

Electrochemical surface treatment is thought to strip off the outer layers, exposing layers of graphite in the core of the fibre, as well as oxidising the graphite. Fitzer and Weiss<sup>21</sup> described the potential active sites on a graphite crystal in their review. The essential point is that crystal basal surfaces of completely bonded carbon atoms (C-planes) are chemically inert, and that reactions take place at incomplete bonded edges and faults in the structure. Mahy *et al.*<sup>22</sup> estimated that the active sites on electrochemically surface-treated Tenex carbon fibres occupy 25% of the surface, assuming that the outer skin is a perfect graphite structure. Our own measurements on Courtaulds XAS carbon fibres put the surface occupation at 5% at the optimum surface-treatment conditions, using a tritium–proton exchange procedure.<sup>12</sup>

Based on the above knowledge and observations, we adopted two carbon fibre models.

**Single-layered graphitic models for carbon fibres.** A diagonal graphitic plane, comprising 52 six-membered rings (in a 4 × 13 configuration) and of 150 carbon atoms, was built as the principal, non-surface-treated carbon fibre model [see Plate 1(a)]. In this structure the carbon atoms have sp<sup>2</sup> hybrid-

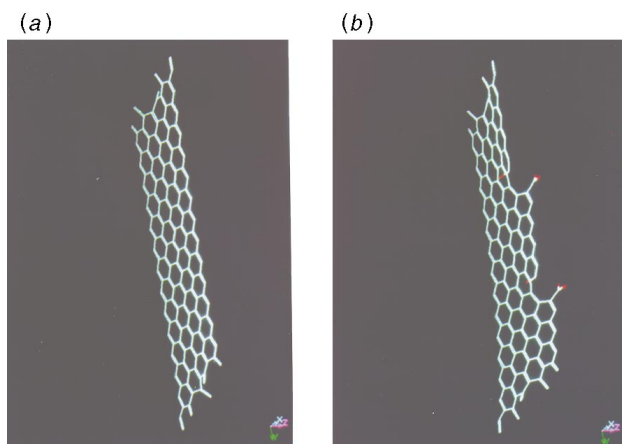


**Plate 1** Structures of the single graphitic plane: (a) as the principal non-surface-treated carbon fibre model, (b) as an example of the surface-treated carbon fibre model, in which the number of functionalities,  $n$ , is 4

isation, and form partial double bonds (the perfect graphitic structure is a flat plane). Those carbons at the outermost edge form CH (in closed rings) or CH<sub>2</sub> (open ends). A further six variants of the model were built based on this structure. Surface treatment was represented by the introduction of hydroxy (OH) and carboxy (COOH) groups: each time, a C–C bond was broken along the edge of the plane, and a pair of OH and COOH groups was added to the graphitic plane [see Plate 1(b)]. The number of broken C–C bonds was gradually increased to six, and consequently six pairs of OH and COOH were introduced into the model. The functional groups were arranged in such a way as to be evenly distributed along the edge of the plane. The model can only accommodate six pairs of functional groups; more breakage of C–C bonds only results in the outer edge being peeled off, and the oxidation of the newly exposed active sites. The total number of active sites is not changed. These structures were then relaxed by molecular mechanics energy minimisation, using conjugate gradients and charges derived from the  $Q_{eq}$  method, until energy convergence (at 0.01 kcal mol<sup>-1</sup>) was achieved.

**Multi-layered graphitic models for carbon fibres.** Three layers of graphitic planes, each comprising 117 six-membered rings (in a 9 × 13 configuration) and of 300 carbon atoms, formed the multi-layer graphitic model [see Plate 2(a)]. The total number of carbon atoms was 900. Non-surface-treated carbon fibres were modelled as three parallel graphitic planes. The functional groups were introduced in the same way as in the

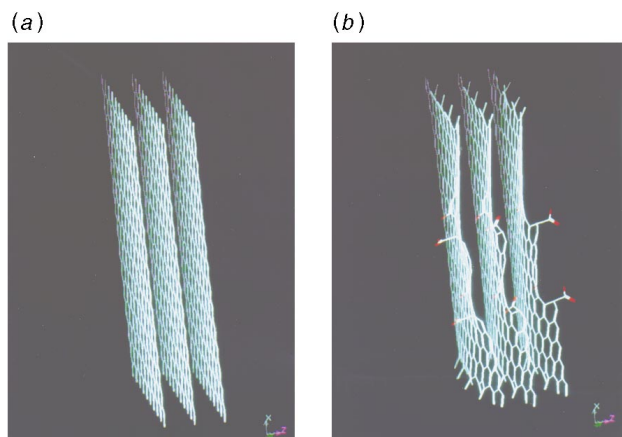


**Plate 2** Structures of the multi-layered graphitic planes: (a) as the principal non-surface-treated carbon fibre model, (b) as an example of the surface-treated carbon fibre model, in which  $n = 4$

single-layer models, *i.e.* evenly, and only distributed along one edge of each plane [see Plate 2(b)]. The distance between the planes was set at 3.35 Å, in accordance with the graphite crystal structure.<sup>23</sup> These structures were also relaxed by molecular mechanics energy minimisation, using conjugate gradients and charges derived from the  $Q_{eq}$  method, until energy convergence (at 0.01 kcal mol<sup>-1</sup>) was achieved.

### Modelling of the linear DGEBA homopolymer chain

A structural repeat unit containing the bisphenol A moiety linked to an opened epoxide ring was constructed with one head and one tail linkage [see Fig. 1(a)]. A homopolymer of ten repeat units was built by linking the heads to the tails (see Plate 3). Polymer torsion angles were set at the default values, taken from the head and tail torsion angle of the monomer model. Although the polymer tacticity control was selected to be isotactic, bond angles at several points along the polymer chain were manipulated to generate a random coil. Both ends were capped by epoxide rings. The polymer chain was then

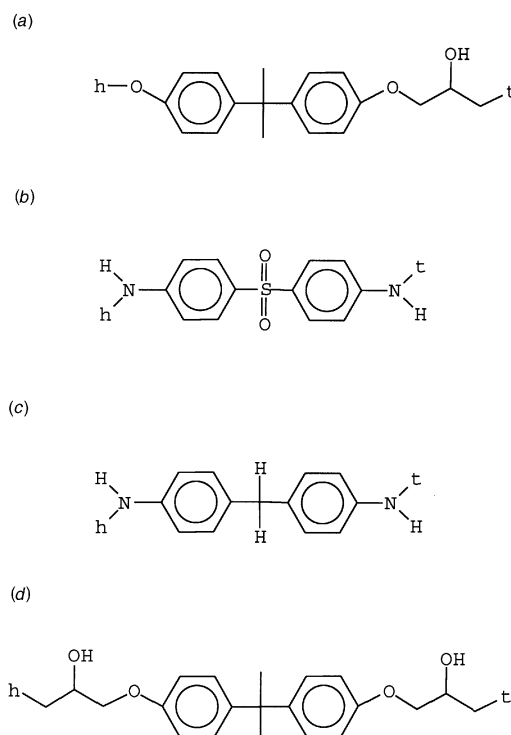


**Fig. 1** Structural repeat units for (a) the diglycidyl ether of bisphenol A (DGEBA) in homopolymer and random copolymers, (b) bis(4-aminophenyl)sulfone (DDS), (c) bis(4-aminophenyl)methane (DDM) and (d) diglycidyl ether of bisphenol A (DGEBA) in alternating copolymers. h = head linkage, t = tail linkage for the polymer builder.

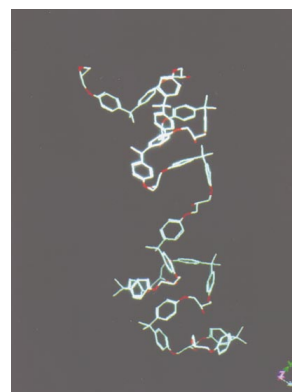


**Plate 3** Structure of the homopolymer model of the diglycidyl ether of bisphenol A

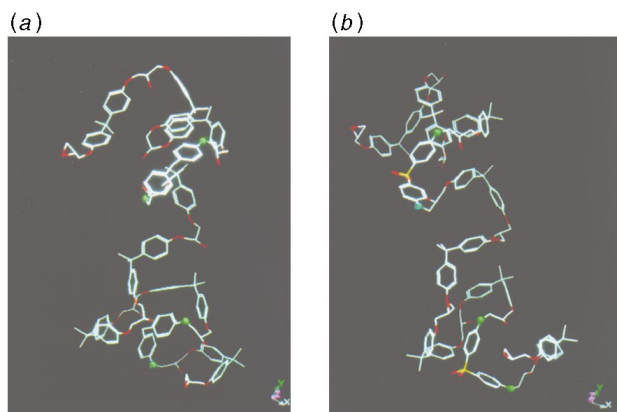


**Plate 4** Structures of (a) a random copolymer of DGEBA-DDM, (b) a random copolymer of DGEBA-DDS

relaxed by molecular mechanics energy minimisation, using conjugate gradients and charges derived from the  $Q_{eq}$  method, until energy convergence (at  $0.01 \text{ kcal mol}^{-1}$ ) was achieved.

#### Modelling of amine-cured epoxy resin

An amine-cured epoxy resin forms a cross-linked structure, with each amine group reacting with two epoxides. Molecular simulation with the Cerius<sup>2</sup> program can only build a linear polymer with one head and one tail linkage. Therefore we used the linear polymer as an epoxy resin model. The different degrees of cross-linking were represented by constructing homopolymer, random copolymers (amine:epoxy, 2:8) and alternating copolymers.

AB copolymers containing the diglycidyl ether of bisphenol A (DGEBA) and the bis(4-aminophenyl)sulfone (DDS) units, were built from the DGEBA structural repeat unit model [see Fig. 1(a,d)] and the DDS structural repeat unit model [see Fig. 1(b)]. AB copolymers containing DGEBA and the bis(4-aminophenyl)methane (DDM) units [see Fig. 1(c)], were built from the DGEBA and DDM structural repeat unit models.

**DGEBA-DDM random copolymer.** Using the random copolymer builder, a DGEBA-DDM random copolymer was constructed. The ratio of DGEBA to DDM was 8:2. One end of the copolymer chain was capped with amine, and the other with epoxide. A total of ten repeating units was used. The polymer chains were then relaxed by molecular mechanics energy minimisation, using conjugate gradients and charges derived from the  $Q_{eq}$  method, until energy convergence (at  $0.01 \text{ kcal mol}^{-1}$ ) was achieved [see Plate 4(a)].

**DGEBA-DDM alternating copolymer.** Using the alternating copolymer builder, a DGEBA-DDM alternating copolymer was constructed. The ratio of DGEBA to DDM was 1:1. One end of the copolymer chain was capped with amine, and the other with epoxide. A total of ten repeating units was used. The polymer chain was then relaxed by molecular mechanics energy minimisation, using conjugate gradients and charges derived from the  $Q_{eq}$  method, until energy convergence (at  $0.01 \text{ kcal mol}^{-1}$ ) was achieved [see Plate 5(a)].

**DGEBA-DDS random copolymer.** The random DGEBA-DDS copolymer was built using the same method as that described for the construction of the DGEBA-DDM random copolymer [see Plate 4(b)].

**DGEBA-DDS alternating copolymer.** The alternating DGEBA-DDS copolymer was built using the method described for the construction of the DGEBA-DDM alternating copolymer [see Plate 5(b)].

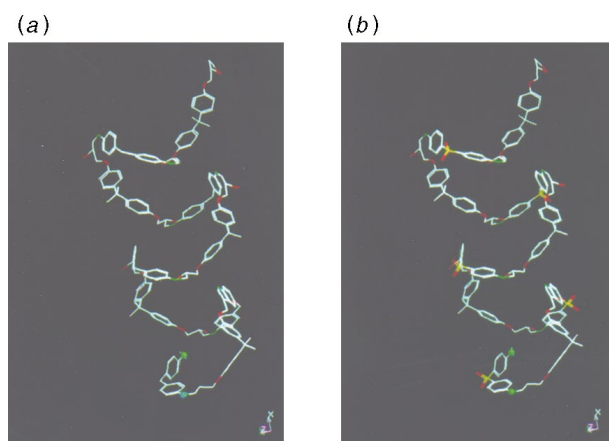


**Plate 5** Structures of (a) an alternating copolymer of DGEBA-DDM, (b) an alternating copolymer of DGEBA-DDS

## Results and Discussion

### The geometry of the graphitic planes

The structures of the single-layered carbon fibre models with functional groups attached were found to deviate from the perfectly flat graphitic plane after energy minimisation. The change in formal valence of the carbons, *i.e.* from  $sp^2$  in graphite to  $sp^3$  in the modified atoms, and the requirement for a bond angle of  $109.5^\circ$  rather than  $120^\circ$ , causes this curvature. More functional groups caused more severe distortions [see Plate 1(b)]. In the oxidised part of the multi-layered models (where functional groups were added), the graphite planes also curved outwards when energy minimisation was performed, while in the non-oxidised part, the graphite structure was not changed [see Plate 2(b)]. The electrostatic repulsion between functional groups on each layer, and the change in formal valence of the modified carbons, contributed to the changes. The distance between the planes in the non-oxidised part remained at  $3.35 \text{ \AA}$ .

### Interactions between single-layered graphitic models and polymers

Interactions of the single-layered model with the DGEBA homopolymer, alternating copolymers and random copolymers are shown in Fig. 2. Obviously, the energy of the interaction depends on many factors, such as the initial structure of the

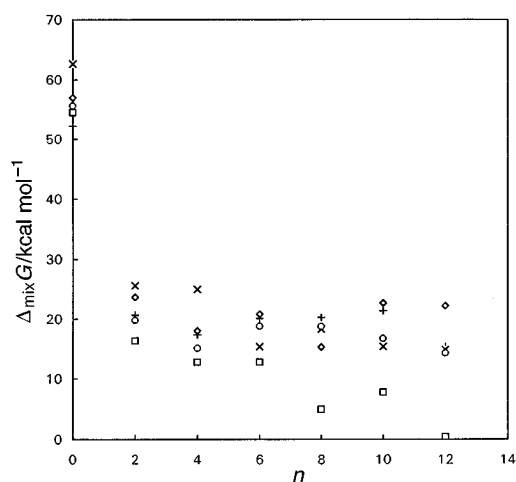


**Fig. 2** Plots of  $\Delta_{mix}G$  vs.  $n$ , representing the interaction of the single-layer models with the DGEBA homopolymer (+), random copolymer of DGEBA-DDS (○), random copolymer of DGEBA-DDM (◇), alternating copolymer of DGEBA-DDS (□) and alternating copolymer of DGEBA-DDM (x)

polymer chain and the size of each model in the binary system. However, once the polymer chain was chosen, its energy term was largely fixed, and any change of the Gibbs energy of mixing is related to the change in the carbon fibre models. Therefore, the energy term is not useful in its absolute value, but in its relative order. Whilst individual plots may show minor differences, they all conform to a general trend, *i.e.* after a marked decrease of 35 kcal mol<sup>-1</sup> from  $n=0$  to  $n=2$  (where  $n$  is the number of functional groups introduced), there is a steady decrease accounting for *ca.* 5–10 kcal mol<sup>-1</sup>. The more functional groups were introduced on the carbon fibre models, the smaller  $\Delta_{\text{mix}}G$  became. The biggest change was observed when the first pair of functionalities was introduced. Further increases in the concentration of functionalities only resulted in small changes in  $\Delta_{\text{mix}}G$ . The implication of a decreasing  $\Delta_{\text{mix}}G$  is that the presence of the functional groups improved the interaction, and hence the compatibility and adhesion, between the carbon fibre model and the polymer chain.

### Interactions between multi-layered graphitic models and polymers

Interactions of the multi-layered model with the DGEBA homopolymer, alternating copolymers and random copolymers are shown in Fig. 3. Owing to the long CPU time needed, calculations were only performed using four of the models with functionalities  $n$  of 0, 4, 6 and 12. Again a similar trend was observed. A decrease of 200 kcal mol<sup>-1</sup> from  $n=0$  to  $n=2$  was recorded, followed by a steady decrease accounting for *ca.* 10 kcal mol<sup>-1</sup>. These observations conform to those made on the single-layer model.

Note that the changes of  $\Delta_{\text{mix}}G$  values calculated from the multi-layer models are larger than from the single-layer models. This is because the initial energies of the 900 atom carbon fibre models are larger and non-polar, and hence less compatible with the polymer than the single-layer model. When treated, defects in and damage to the graphitic plane occur, which then allow the polymer to interact with smaller graphitic planes, and therefore improve the adhesion. It may also be rationalised that, for the same  $n$ , there are three times more functional groups in the multi-layer model, which can give rise to better interactions. For the multi-layered graphitic structure, the thickness is now large enough to allow interactions between the lateral face of the graphitic cluster and the polymer, the former now also being a surface. In the molecular pairs needed for the calculation of  $E_{ij}$ , the polymer is placed on the side of the surface, interacting with the three extremities of the gra-

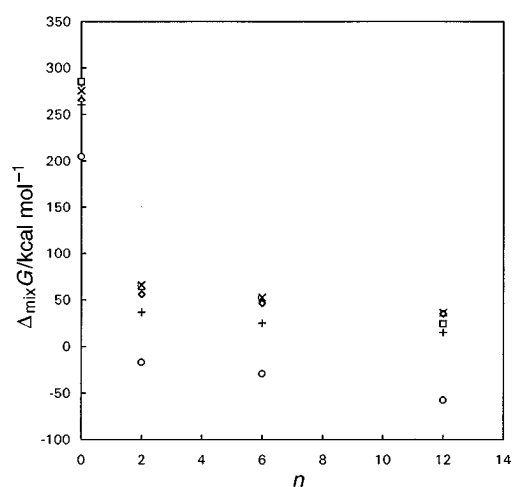


Fig. 3 Plots of  $\Delta_{\text{mix}}G$  vs.  $n$ , representing the interaction of the multi-layer models with the DGEBA homopolymer (+), random copolymer of DGEBA-DDS (○), random copolymer of DGEBA-DDM (◇), alternating copolymer of DGEBA-DDS (□) and alternating copolymer of DGEBA-DDM (x)

phitic plane. This could give rise to stronger interactions than the single-layered model. When the functional groups are present the interaction could be even stronger.

### Comparison of simulation and experimental results

Marshall *et al.*<sup>13</sup> and Baillie and Bader<sup>14</sup> studied the effect of surface treatment of the carbon fibre on epoxy resin composite mechanical properties, especially the interlaminar shear strength (ILSS). Both groups found that surface treatment improves adhesion at the interfaces. However, ILSS reaches a plateau at some stage of the surface oxidation, and further treatment did not result in an increase of the oxygen content on the surface, nor in an increase in the ILSS. We observe similar trends in the calculated data from both carbon fibre models. Soni *et al.*<sup>24</sup> investigated the ILSS of carbon fibre-reinforced epoxy resin composites, and found that the DDS-cured resin had marginally better adhesion than the DDM-cured epoxy resin. He argued that DDS has the rigid  $-\text{SO}_2-$  linkage, and thus imparted better rigidity to the final cross-linked structure. Our calculation was not able to reflect this phenomenon.

### Conclusion

This work demonstrates that the molecular modelling method, BLENDS, can be used to simulate the non-covalent bonding interaction with various amine-cured epoxy polymer models. Two carbon fibre models were proposed and both are valid. Amine-cured epoxy polymer models were modelled as homopolymers, alternating copolymers and random copolymers.  $\Delta_{\text{mix}}G$  was used to indicate the interaction, and hence the interfacial adhesion. The results show a trend, in relation to the level of surface treatment, in agreement with published experimental data on the composite interfacial strength (ILSS). It also provides a fundamental understanding of the mechanism of adhesion at the carbon fibre-reinforced composite interfaces.

We wish to thank the EPSRC for funding (grant number GR/H95891) a postdoctoral research fellowship (S. Y. L.). We also thank Mr. D. Tilbrook for his help with the use of the computational techniques. The referees' comments are also gratefully acknowledged. The results published were generated using the program Cerius<sup>2</sup>. This program was developed by Molecular Simulations Inc.

### References

- 1 J. D. H. Hughes, *Composites Sci. Technol.*, 1991, **41**, 13.
- 2 W. W. Wright, *Composite Polymers*, 1990, **3**, 231; 1990, **3**, 258.
- 3 C. A. Baillie, PhD Thesis, University of Surrey, and references therein.
- 4 Information on the XPS analysis of treated carbon fibre surfaces is abundant in the literature, *e.g.*: C. Kozłowski and P. M. A. Sherwood, *J. Chem. Soc., Faraday Trans. 1*, 1984, **80**, 2099; R. H. Bradley, X. Ling and I. Sutherland, *Carbon*, 1993, **31**, 1115; I. Hamerton, J. N. Hay, B. J. Howlin, J. R. Jones, S. Y. Lu, G. A. Webb and M. G. Bader, unpublished results.
- 5 J. M. Barton, G. J. Buist, A. S. Deazle, I. Hamerton, B. J. Howlin and J. R. Jones, *Polymer*, 1994, **35**, 4326; I. P. Aspin, J. M. Barton, G. J. Buist, A. S. Deazle, I. Hamerton, B. J. Howlin and J. R. Jones, *J. Mater. Chem.*, 1994, **4**, 385; A. S. Deazle, C. R. Heald, B. J. Howlin, I. Hamerton and J. M. Barton, *Polym. Prepr., Jpn. (Engl. Edn.)*, 1995, **44**, E11; I. Hamerton, C. R. Heald and B. J. Howlin, *Macromol. Theory Simul.*, 1996, **5**, 305.
- 6 J. W. Holubka, R. A. Dickie and J. C. Cassatta, *J. Adhesion Sci. Technol.*, 1992, **6**, 243.
- 7 L. H. Lee, *J. Adhesion*, 1994, **46**, 15.
- 8 A. R. Tiller and B. Gorlla, *Polymer*, 1994, **35**, 3251.
- 9 D. Attwood and P. I. Marshall, *Composite*, 1996, **27A**, 775.
- 10 A. Calderone, V. Parente and J. L. Bredas, *Synth. Met.*, 1994, **67**, 151.
- 11 D. J. Johnson, in *Chemistry and Physics of Carbon*, ed. P. A. Thrower, Marcel Dekker, New York, 1984, vol. 20, p.1.

- 12 I. Hamerton, J. N. Hay, B. J. Howlin, J. R. Jones, S. Y. Lu, G. A. Webb and M. G. Bader, *ECCM-7, Proceedings of the Seventh European Conference on Composite Materials, London 1996*, Woodhead Publishing Ltd., Cambridge, 1996, vol. 2, p. 435.
- 13 P. I. Marshall, D. Attwood and M. J. Healey, *Composites*, 1994, **25**, 752.
- 14 C. A. Baillie and M. G. Bader, *J. Mater. Sci.*, 1994, **29**, 3822.
- 15 M. Blanco, *J. Comput. Chem.*, 1991, **12**, 237; C. F. Fan, B. D. Olafson, M. Blanco and S. L. Hsu, *Macromolecules*, 1992, **25**, 3667.
- 16 *Computational Instruments Property Prediction User's Reference*, Cerius<sup>2</sup>, v.1.6, Molecular Simulation Inc., 1994.
- 17 S. L. Mayo, B. B. Olafson and W. A. Goddard III, *J. Phys. Chem.*, 1990, **94**, 8897.
- 18 A. K. Rappe and W. A. Goddard III, *J. Phys. Chem.*, 1991, **95**, 3358.
- 19 M. Guigon and A. Oberlin, *Composites Sci. Technol.*, 1986, **27**, 1.
- 20 E. J. Roche, J. G. Lavin and R. G. Parrish, *Carbon*, 1988, **26**, 911.
- 21 E. Fitzer and R. Weiss, *Carbon*, 1987, **25**, 455.
- 22 J. Mahy, L. W. Jenneskens, O. Grebandt, A. Venema and G. D. B. Van Houwelingen, *Surf. Interf. Anal.*, 1994, **21**, 1.
- 23 F. A. Cotton, G. Wilkinson and P. L. Gaus, *Basic Inorganic Chemistry*, 3rd edn., Wiley, New York, 1995.
- 24 H. K. Soni, R. G. Patel and V. S. Patel, *Makromol. Chem.*, 1993, **211**, 1.

*Paper 6/04782C; Received 8th July, 1996*